communications earth & environment

Article

A Nature Portfolio journal

https://doi.org/10.1038/s43247-026-03279-4

Increased contributions of climate-driven wildfires to nitrogen deposition in the United States

Patrick C. Campbell [1,2] ✉, Daniel Q. Tong [1,2,3], Shinkuang Chang[3], Siqi Ma[3], Yunyao Li [3,4], Jiaxin Ding[3], Rick Saylor [2], Barry Baker [5], Youhua Tang[1,2] & John Walker[6]

Climate change and increases in the frequency and severity of climate-driven wildfires, particularly in the western United States, has serious ramifications for enhanced downwind reactive nitrogen (Nr) emissions, deposition, and critical load exceedances. Here we present a multi-decadal (2002 – 2021), harmonized model-data-driven study using the George Mason University North American Chemical Reanalysis (NACR) system and simulations including both "with-fire" and "without-fire" conditions to quantify the change in trends of fire activity and source contributions to total Nr emissions and deposition over the U.S. Our results show that fire activity has increased substantially in the western U.S., especially in the west-northwest U.S. for wildfires, and that this increase is associated with positive annual near-surface temperature and vapor pressure deficit anomalies compared to the period average. Major results and implications of this work are increasing trends in the contribution of climate-driven wildfires to higher Nr emissions, deposition, and critical load exceedances of up to 20-40% due to fires in the western U.S. There are also smaller increases (<5 %) in Nr deposition trends for the eastern U.S., which are related to greater occurrence and reporting of agricultural and prescribed burns.

Improved understanding of the complex nitrogen (N) cycle (i.e., fixation, mineralization, nitrification, immobilization, and denitrification) is essential because N is the crucial nutrient for sustaining life in our Earth system. Due to the availability and necessity of fertilizers to sustain growing food production and population, excess fluxes of N to sensitive terrestrial and aquatic ecosystems can have detrimental effects such as acidification and eutrophication[1]. Furthermore, both anthropogenic and natural sources of nitrogen oxide (NO_x) emissions, which consist of both nitric oxide (NO) and nitrogen dioxide (NO_2), as well as gaseous ammonia (NH_3) emissions mainly from anthropogenic sources, largely perturb the N budget and cycle.

The total nitrogen oxide (NO_x) emissions in the contiguous U.S. (CONUS) have annually decreased from about 25 million tons in 2002 to 10 million tons in 2017[2]. These NO_x sources (consisting of anthropogenic + fires) are dominated (~90% of the total) nationally by electric generating utilities, on-road and non-road mobile sources, and other point- and nonpoint-based fuel combustion sources such as industry from the U.S. EPA's national emissions inventory (NEI)[2]. This further implies that ~10% of the total NO_x is contributed by fires, which amounts to ~1 million tons in 2017. The anthropogenic emissions are projected to further decline due to the increased fuel efficiency and tighter standards that are proposed to continue in the coming decades[3,4] Meanwhile, ammonia (NH_3) emissions are relatively unregulated, largely dominated by agricultural sources (~90% of the total), and have remained steady at over 4 million tons nationally from 2002 to 2017[2]. Future projections suggest that such agricultural NH_3 emissions sources will increase nationally by 2040[3,4].

In the face of climate change and increases in the size and severity of wildfires both regionally and globally, related NO_x and NH_3 emissions changes have stark consequences for perturbing the N cycle and the "nitrogen cascade"[5–9]. While criteria air pollutant emissions, such as NO_x in most of the U.S. have decreased in past decades due to environmental

[1]Center for Satellite and Earth Science Research, Cooperative Institute for Satellite Earth System Studies, George Mason University, Fairfax, VA, USA. [2]Air Resources Laboratory, National Oceanic and Atmospheric Administration, College Park, MD, USA. [3]Atmospheric, Oceanic & Earth Sciences Department, George Mason University, Fairfax, VA, USA. [4]Department of Earth and Environmental Sciences, University of Texas at Arlington, Arlington, TX, USA. [5]National Weather Service, Environmental Modeling Division, National Oceanic and Atmospheric Administration, College Park, MD, USA. [6]Center for Forest Watershed Research, Coweeta Hydrologic Laboratory, U.S. Department of Agriculture Forest Service, Otto, NC, USA. Retired: Shinkuang Chang, Rick Saylor.
✉e-mail: pcampbe8@gmu.edu

regulations and technological advances[2], there is evidence of an increased contribution of fire emissions to the total NO_x and NH_3 emissions in the U.S. that contribute to degraded air quality, increased N deposition, and consequential human and ecosystem health impacts, especially in wildfire-prone areas in the west-northwest U.S.[10–13]. For example, increases in total reactive N (Nr; composed of both oxidized NO_x and nitrous oxide; N_2O, as well as reduced forms like NH_3 and ammonium NH_4^+, i.e., NH_x=NH_3 + NH_4^+) deposition were found to be as large as 6-12 times the critical load (CL) threshold for major forests in California during the historic 2020 wildfire season in the U.S.[13].

A CL serves as a crucial environmental threshold, specifically defined as the maximum amount of anthropogenic N deposition that an ecosystem can withstand without experiencing detrimental effects[14]. These detrimental effects can manifest in various ways, encompassing both qualitative and quantitative changes within diverse ecosystems. Qualitatively, the exceedance of a CL can lead to the loss of biodiversity. This might involve a reduction in species richness, alterations in community composition, or the decline of sensitive indicator species. Such shifts can have cascading impacts throughout the ecosystem, affecting food webs and overall ecological stability. Quantitatively, CLs are often established through empirical evidence, relying on scientific research and long-term monitoring to identify specific levels of N deposition that trigger measurable negative impacts. For example, excessive N can lead to soil acidification, nutrient imbalances (e.g., phosphorus limitation due to increased nitrogen), changes in water chemistry and eutrophication, and increased susceptibility to disease or insect outbreaks in vegetation[14]. The concept of a CL is fundamental to environmental policy and legislative efforts aimed at mitigating the impacts of N pollution. For example, legislation for the National Atmospheric Deposition Program (NADP) monitoring network (established in 1977) and CLs has evolved primarily under the U.S. Clean Air Act (CAA).

However, there remain inherent difficulties in consistently observing or modeling Nr species and their fluxes across the land/biosphere and atmosphere, and there are limited studies that have been able to effectively quantify the changes in climate and anthropogenic and wildfire emission sources on Nr deposition and terrestrial ecosystem endpoints over the past decades[12,13]. The lack of studies on the shifting emission paradigm between anthropogenic and natural processes, such as wildfires, remain as glaring uncertainties with respect to the impacts on downwind atmospheric Nr deposition and the impacts to sensitive terrestrial ecosystems across the world[14–20].

This knowledge gap demands a better understanding of the long-term (~multi-decadal) fire activity and implications on changes in Nr emissions, deposition, and the impacts on downwind ecosystems across CONUS. To aid in this important effort, here we apply the George Mason University North American chemical reanalysis (NACR) system that consists of two, state-of-the-science 20-year (2002–2021) coupled weather-chemical transport model (CTM) simulations both "with-fire" and "without-fire" impacts to quantify the change in relative trends and contributions of fire sources to the total Nr emissions and deposition trends over CONUS. We hypothesize that trends in fire activity, emissions and resulting atmospheric nitrogen deposition to downwind ecosystems are related and has substantially changed in recent decades, where our objectives are to use the harmonized long-term data and model simulations to perform comparative Nr deposition trend analyses and assess impacts on CLs over the past 20 years. Results here show that there are increasing trends in the contribution of climate-driven wildfires to higher Nr emissions, deposition, and CL exceedances of up to 20–40% due to fires in the western U.S.

Results and discussion

Climate-wildfire activity and trends

Climatic conditions, such as 2-meter temperature (TEMP2) and vapor pressure deficit (VPD; the amount of moisture missing from the atmosphere compared to saturation) are highly correlated with wildfire activity and burned areas in both forested and non-forested areas of the U.S. (see "Methods"; Supplementary Fig. S1 and Table S1 for explanation of dominant vegetation/land use used in NACR), with higher TEMP2 and VPD being associated with higher fire activity[20–22]. Here we compare climate warming stripes, annual values, and trends for the total annual wildfire acres burned anomalies (compared to the 2002–2021 average) based on the EQUATES and EPA NEI emissions and modeling platform, against the annual average anomalies for NACR simulated TEMP2 and VPD in the western U.S. NOAA climate regions (Fig. 1). See "Methods"; Supplementary Figs. S2 and S3 that describe the delineation of NOAA climate regions along with 2002–2021 average TEMP2 and total precipitation amounts for each region and calendar month.

There is very close agreement in annual positive (negative) anomalies between wildfire acres burned and positive (negative) anomalies in TEMP2 and VPD, especially in west (WC), northwest (NWC), and southwest climate (SWC) regions (Fig. 1A–C). There is an apparent shift in the second half of the NACR record (after year 2011) where WC, NWC, and SWC fire climate regions experience increased occurrence of positive wildfire acres burned anomalies, peaking in years following 2017-2018. This coincides with warmer TEMP2 and positive VPD anomalies for 2012–2018 compared to 2002–2011 in the western U.S. There is a statistically significant increasing trend for TEMP2 anomalies between 2002 and 2021 for the west WC, SWC, and NWC regions as indicated by the Mann–Kendall (MK) scores between about 0.88–0.96 (i.e., close to 1 with trends very confident) and Theil–Sen (TS) trends of 0.04–0.06 °C/year (See insert MK and TS scores in Fig. 1. as well as Supplementary Table S2 and "Methods" section for more description of MK and TS). While MK scores are lower for wildfire acres burned, wildfire activity (see Table S2), and VPD anomalies (except in WC, with higher VPD MK of 0.97) they remain significant with strong positive trends in the WC and NWC at about 2.1×10^5–2.2×10^5 acres burned/year, and 0.01–0.04 hPa/year, respectively (Fig. 1A, B; Tables S2 and S3).

There is a sharp drop in wildfire activity and acres burned in 2019 that is associated with much cooler and negative VPD anomalies across all western U.S. climate regions. The wildfire activity, warmer TEMP2, and positive VPD anomalies rebound after 2019 (both for 2020 and 2021), where there is also a peak in the positive anomalies for wildfire acres burned in 2020 for these western regions, especially for the WC (Fig. 1A and Supplementary Fig. S4a) associated with the August complex fires[13]. There is less significant wildfire, TEMP2, and VPD trends in the northern plains climate (NPC) region, with low MK and TS scores.

There is a clear compensation of the positive wildfire anomalies by negative anomalies in the following years, especially in the NWC and NPC regions (Figs. 1B, D). Wildfires, by definition (necessity to accumulate fuel loads), cannot spread linearly over time, and the data in Fig. 1 shows a cyclical phenomenon with a period of about 2–4 years in the NWC and NPC embedded in the long-term average trends strongly in sync with associated regional TEMP2 and VPD changes. These regions, most prolifically the NPC (with the strongest apparent oscillation in wildfire anomalies), have a larger proportion of land area characterized by low-lying grasslands compared to other regions of the west (Supplementary Fig. S1) that tend to have relatively fast wildfire recovery times, sometimes within a few years. Thus, a complex interplay exists between long-term climate trends, regional weather changes, and post-wildfire fuel load recovery periods.

Prior to 2014 in the eastern U.S., the wildfire activity and acres burned anomalies oscillate about zero in conjunction with TEMP2 and VPD (Supplementary Figs. S4b and S5), with minimal discernible trends. However, there are increases in positive wildfire anomalies after about 2014 in conjunction with sharp increases in TEMP2 and VPD until 2018, especially in the south (SC) and southeast climate (SEC) regions. Overall, there are clear downward trends in wildfire acres burned in the east (Fig. S4b), with significant MK scores (0.88–0.98) and TS values of about -9×10^3 to -8×10^5 acres burned/year (Table S3). This demonstrates that over time wildfire size has been decreasing in the eastern U.S., despite weak positive trends of TEMP2 and VPD (MK scores mainly below ~0.5) for most climate regions (Supplementary Table S4). There are important differences in the dominant fuel types (mixed hardwoods) and topography/regional climate conditions (flat and humid conditions) in the east compared to the western

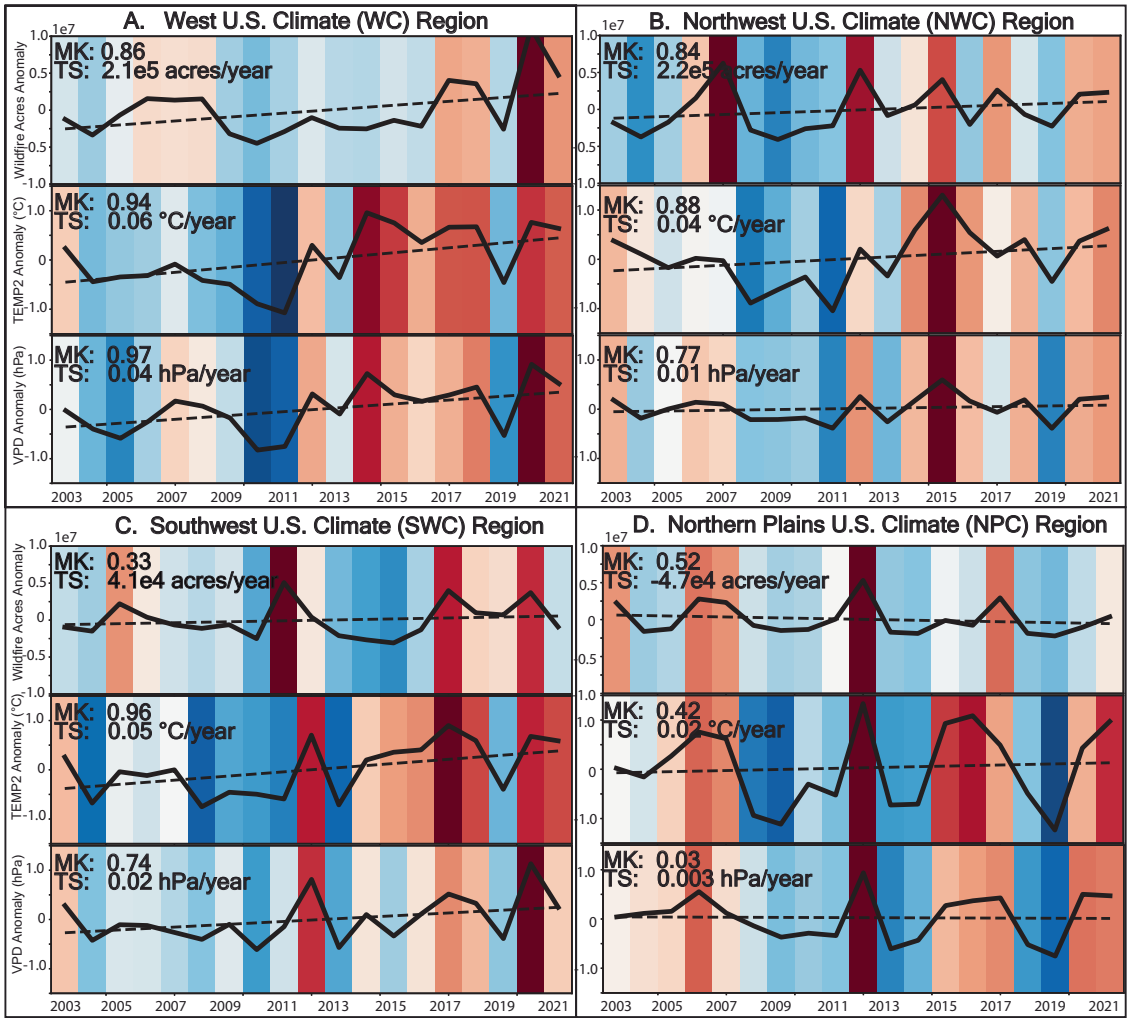

Fig. 1 | Warming stripes and trends in wildfires and climate. Warming stripes, annual values (solid lines), and trends (dashed lines) for annual 2002–2021 total wildfires acres burned anomaly, TEMP2 anomaly (degrees C), and VPD anomaly (hPa) for the western U.S. fire climate regions (see Supplementary Fig. S2 for regions describing **A** NPC, **B** SWC, **C** NWC, and **D** WC). Cooler colors (including white to blues) indicate negative anomalies, while warmer colors (white to pinks and reds) indicate positive anomalies compared to the period average. Insert values pertain to Mann–Kendall (MK) scores and Theil–Sen (TS) trends across the western U.S (see "Methods" below for explanation of MK and TS). Here we note that the EQUATES dataset does not explicitly report the 2002 year's point source fires, and thus values are removed from analysis for that year. Warming stripe analyses are based on Ed Hawkins' "temperature changes around the world (1901–2018)" available at https://showyourstripes.info/s/globe. Source code based on https://docs.dkrz.de/doc/visualization/sw/python/source_code/python-matplotlib-warming-stripes-and-trend.html.

U.S (Table S1). Hence, the different climate-driven wildfire trends in the east (compared to the west) are driven by regional climate shifts that include increasingly heavy precipitation events over the east between 2002 and 2021[15] and decreasing wildfire sizes over this period.

Climate-wildfire impacts on reactive nitrogen emissions

Considering the strong relationships between increasing trends in climate indicators, such as TEMP2, VPD, and wildfire activity/acres burned in the western U.S. climate regions (see Figs. 1; S4; Supplementary Tables S2 and S3), we hypothesize that there are also shifts in the trends in contributions of wildfires to total Nr emissions as well as a relationship between VPD and wildfire Nr (i.e., NO_x and NH_3) emissions between 2002 and 2021. There is a prominent contribution of wildfire NO_x and NH_3 emissions between 2002 and 2017 in the western U.S., e.g., accounting for up to ~10–20% and 20–30% of the total emissions in the NWC region. In other western climate regions, the wildfire emissions contribution to the total is lower and ranges from ~5 to 10% for NO_x and 5–15% for NH_3. Trends in wildfire NO_x and NH_3 emission contributions agree with increasing wildfire activity between 2002 and 2017 (Fig. 1), with subsequent corresponding decreases in 2018–2021.

A linear regression analysis of wildfire Nr ($NO_x + NH_3$) emissions versus VPD for western climate regions shows linear increases in wildfire Nr emissions with increasing VPD, with strong Pearson correlation coefficients (r) of about 0.7 in the WC and SWC regions (Fig. S6a, b). The strong correlation suggests a connection between higher VPD, drier fuels, and an association with wildfire Nr emissions behavior changes in the WC and SWC regions. Linear correlations between wildfire Nr emissions and VPD are smaller, but remain moderately strong for NWC and NPC (r ~ 0.5–0.6; Fig. S6c, d).

Fire-induced reactive nitrogen deposition and trends

Total (wet + dry) Nr deposition in NACR contains both oxidized (NO, NO_2, nitric acid (HNO_3), dinitrogen pentoxide (N_2O_5), chlorine nitrate ($ClNO_3$), and particulate nitrate (NO_3^-)) and reduced forms (NH_3 and NH_4^+) of nitrogen:

$$Nr = NO + NO_2 + HNO_3 + N_2O_5 + ClNO_3 + NO_3^- + NH_3 + NH_4^+$$

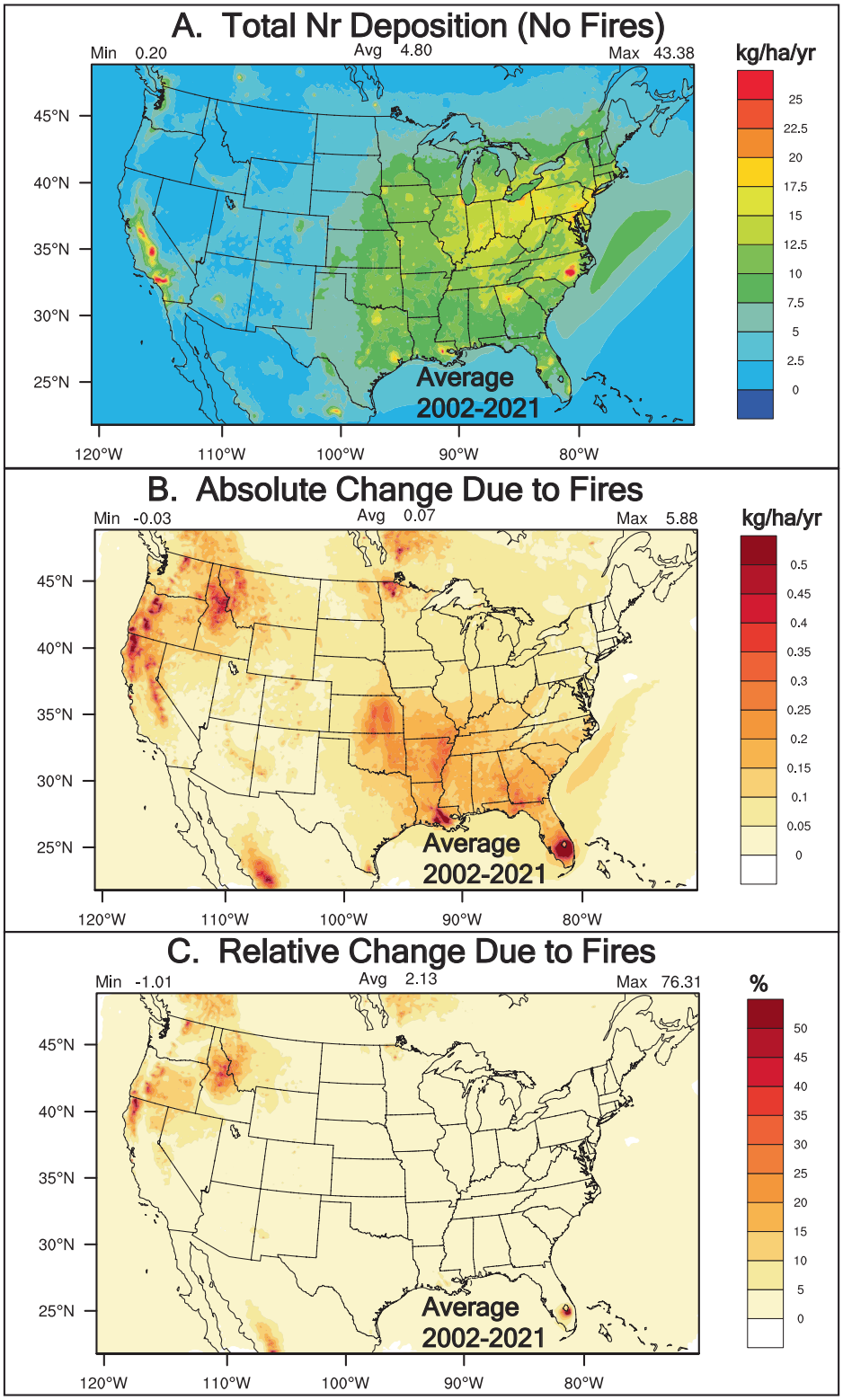

Fig. 2 | Spatial patterns of annual total Nr deposition. Annual 2002–2021 average total reactive N (Nr) deposition for **A** absolute (kg/ha/yr) total (wet + dry), **B** absolute (kg/ha/yr) difference (FIRE-NOFIRE), and **C** relative (%) difference (FIRE-NOFIRE/NOFIRE).

The particulate NO_3^- and NH_4^+ are included in NACR based on a modal aerosol distribution for all three modes (i.e., Aitken, accumulation, and coarse), where reduced NH_x=NH_3 + NH_4^+. Comparison of the 2002–2021 average annual spatial FIRE (wildfire + prescribed + agricultural) vs. NOFIRE (i.e., all fire emissions removed) NACR simulations (see "Methods" for model configuration and simulation design) demonstrates that the presence of fires leads to profound increases (max grid cell increase ~+6 kg/ha/yr) in total Nr deposition across the U.S. in terms of absolute changes (Fig. 2). We note that previous sections focused on the climate–wildfire interactions, and here the Nr deposition sensitivity simulations include all fire sources removed. Given computational constraints, we do not include additional three sensitivity runs (i.e., with each fire sector removed); however, the largest relative fire-induced Nr deposition trends are predominantly due to climate-driven wildfire sources in the western U.S. (Fig. 2C), which remains a focal point of the results.

The overall decreasing total Nr deposition trends for both FIRE and NOFIRE NACR simulations (Fig. S7) first confirms well-understood patterns between 2002 and 2021 that are a result of reductions in anthropogenic NO_x emissions due to air quality control and regulations employed across this period[2–4]. The largest absolute increases include areas not typically common for such high Nr deposition, including the west-northwest due to wildfires, and in the south-central and southeast U.S. due to agricultural and prescribed burns (Fig. 2A, B). The largest relative Nr deposition increases due to wildfires (max grid cell increase ~+76%) are found in the west (WC) and northwest (NWC) regions(Fig. 2C).

There is a relative flattening of the overall Nr deposition trends only in the NACR FIRE compared to NOFIRE simulations, especially in the WC and NWC regions after 2011 (see Fig. S7a, dashed vs. solid lines). This is emphasized via analysis of the relative difference between the FIRE-NOFIRE total Nr deposition trends, which conversely shows a strongly increasing trend, MK scores very close to 1 in all western climate regions, and TS trends as large as a 0.5–1% increase in Nr deposition per year due to wildfire sources in the WC and NWC (Table S5). By the year 2020, the increasing fire contributions to Nr deposition trends reach as high as ~20% and 40% in the WC and NWC, respectively (Fig. S7b).

There are also increasing Nr deposition trends in the eastern U.S., however, they are much smaller (mainly <5%) in magnitude depending on the specific climate regions (Figs. 2; S8 and Table S6). This increasing trend in the east is driven by overall decreasing NO_x and NH_3 emissions (dominated by anthropogenic sources) that are coincident with increasing relative amounts of NO_x and NH_3 emissions from fire sources. This is due to increased occurrence and reporting of agricultural and prescribed burning across the U.S. since 2011[23], particularly in the southeast U.S as a means to adapt to climate changes[24]. We note that this shift in reporting is apparent in the trends of agricultural + prescribed burning fire NO_x emissions, comparing the EQUATES 2002–2017 to the other NEI years for 2018–2021, with a stark increase in 2018 for the percent contribution of agricultural + prescribed burning to the total NO_x fire emissions in both the eastern and western U.S.

There is a negative relative (%) difference in the year 2010 that is anomalous to the overall trends for both the west and east U.S. climate regions (Figs. S7 and S8). Other analyses of the NACR simulations shows this is due to relatively larger enhancements in ozone formation during a perpetually dry 2010 during the cool seasons of winter and spring (e.g., February–May), particularly in the east-southeast U.S. These conditions of widespread higher ozone and related NO_z forming compounds (i.e., NO_y-NO_x), in conjunction with relatively low fire activity and NO_x emissions from prescribed and agricultural burns in the east, consequently resulted in overall lower Nr deposition (mainly then from lower NO_2 concentrations) for the FIRE vs. NOFIRE case in 2010. This case in context to overall trends further demonstrates the intrinsic and complex link between fires, Nr, and near-surface air pollution, including connections with ozone formation.

In both the east and west climate regions, there is a strongly increasing trend in total (wet + dry) NHx/Nr deposition ratio, but simultaneously a decreasing trend in total OxN/Nr deposition ratio. The increasing trend in contribution to Nr deposition from fires (mainly wildfires) in the western U.S. is dominated by the reduced NH_x species, with up to an 80% NHx/Nr increase and 18% OxN/Nr decrease in the NWC region due to fires (Supplementary Fig. S9; Tables S7 and S9). This NH_x deposition trend is mainly a result of increases in dry deposition, with much smaller contributions from fires to increasing OxN dry deposition (Supplementary Fig. S13 and Table S11). In the west U.S., there are negative wildfire contributions to the *wet deposition* of Nr (both from NH_x and OxN; Supplementary Table S12), which indicates that increasing wildfire contributions lead to more partitioning (out of total Nr deposition) towards dry deposition, primarily as NHx (and NH_3 due to inherently more rapid dry deposition rates) in the WC and NWC regions. This is also impacted by increasingly drier, higher positive trends in VPD anomalies (Fig. 1) associated with both lower precipitation and lower Nr wet deposition contributions in the parts of the west climate regions.

In the east U.S., there are less discernible trends for contributions of fire sources to deposition of Nr, NHx/Nr, and OxN/Nr in terms of shifting dry vs. wet deposition partitioning to the total, with relative % fire contributions of <2% for Nr wet deposition (Supplementary Fig. S14) and very small relative % changes for dry vs. wet Nr deposition per year from fires (Supplementary Tables S13 and S14). There is indication of overall increasing trends for NHx dry deposition vs. wet deposition; however, the relative % fire contributions for NHx dry deposition remains <10% (Fig. S15) and is even lower (<2%) for OxN dry deposition (Fig. S16).

We presented the relative fire changes to the partitioning of Nr (between OxN and NHx) ratios for both dry and wet deposition, with some demonstrating relative negative changes; however, if presented in terms of absolute changes the FIRE simulations have positive contributions to Nr, OxN, and NHx dry and wet deposition for all years (except 2010 for reasons described above), most prolifically for enhanced NHx dry deposition due to wildfires in the west.

Implications for downwind ecosystems

Climate change and enhanced wildfire activity and emissions lead to strong perturbations in the atmospheric N cascade, which can have profound implications for downwind ecosystems, particularly compared to critical load (CL) thresholds for different ecosystems[13–20]. Here we perform comparisons of the trends in annual average ratio of total Nr deposition (kg-N ha^{-1} yr^{-1}) to a low-end (conservative) CL of 3.1 kg-N ha^{-1} yr^{-1} above which results in detrimental impacts on sensitive lichen species in major forests, and against a CL of 6.2 kg-N ha^{-1} yr^{-1} above which there are potential declines in herbaceous plant species. These approximate CL thresholds represent the dominant terrestrial ecosystem types near and downwind of western U.S. wildfires and are based on a compilation of CL datasets used in a previous study (and from references found within) compared against an ensemble of chemical transport models[25]. In our analysis, the NACR Nr deposition values are compared with the CL thresholds across the different major USGS land use types at each model grid cell and then averaged over the different climate regions (Fig. 3). Although the ratio of Nr/CL (where Nr/CL > 1 represents approximate CL exceedances) has substantially declined between 2002 and 2021 (a testament to more stringent regulations and reduced anthropogenic emissions, see discussions in previous sections), increasing contributions of wildfires to Nr deposition (primarily through increased NH_3 dry deposition) lead to an increase of up to 20% and 40% in Nr/CL ratio for WC and NWC regions, respectively (Fig. 3). This results in flattening of the overall decreasing Nr/CL trends, especially after year 2011 (see dashed lines in Fig. 3A), driving the Nr/CL ratio closer to or even greater than 1 especially for the WC (MK ~1 and TS trends increasing at ~0.6% yr^{-1}) and NWC regions (MK ~1 and TS trends increasing at ~1.2% yr^{-1}) (Fig. 3 and Table S15).

We note that Nr/CL trends relative to the fire contributions (Fig. 3B) is very close to the trends in total Nr deposition in the western U.S. that are driven by increased contributions from wildfires (Fig. S7b). This is because of using effectively static CLs over major forest types and herbaceous plants land use during the 2002–2021 period, where including changes in land use and shifting CLs over time in the NACR simulation domain and climate regions (outside the scope here) would result in additional differences between total Nr and Nr/CL ratios. This also applies for the eastern U.S. climate regions, where the much smaller increases (<5%) in Nr deposition (Fig. S8) are also very similar to the Nr/CL trends, which are impacted by increased occurrence and reporting of agricultural and prescribed burning (especially after year 2018). These topics of shifting land use and human activity related to changes in burning practices as it relates to Nr deposition and CLs are possible future investigations.

As climate change and increases in wildfire trends continue, sensitive ecosystems in some regions of the U.S. will face further enhancements in Nr deposition and potential CL exceedances. These results and NACR data can thus be further used to assess potential implications for specific ecosystem,

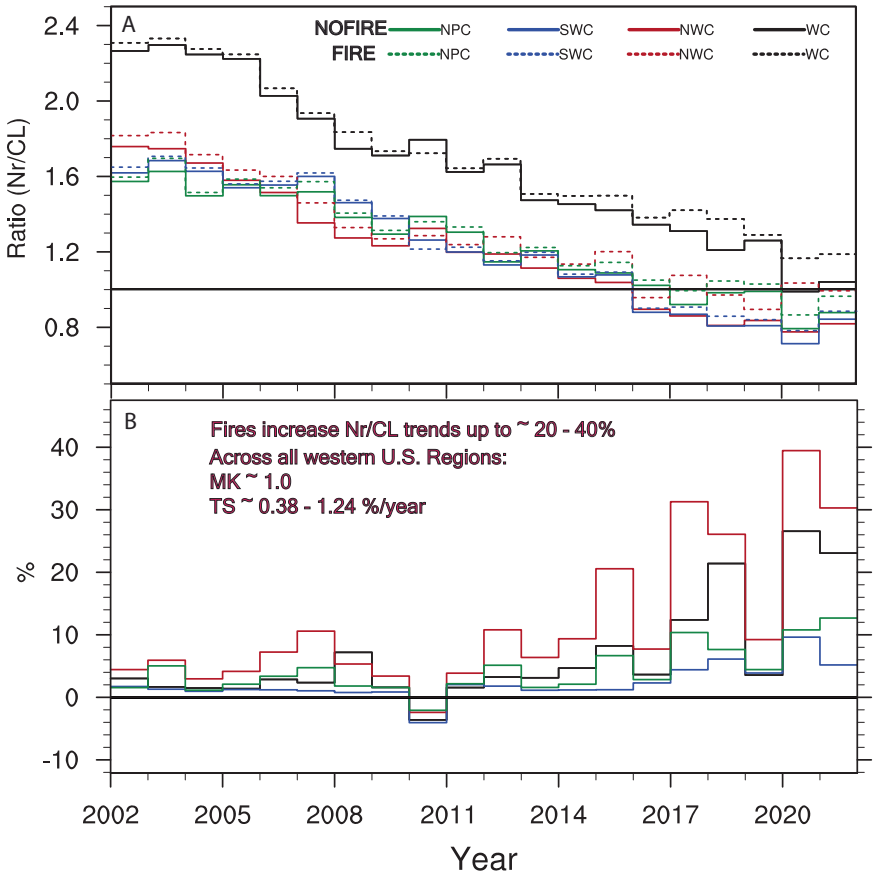

Fig. 3 | Trends in the Nr/CL ratio and contributions from fires. Trends in **A** annual average ratio of total Nr deposition (kg-N ha^{-1} yr^{-1}) to a low-end (conservative) CL of 3.1 kg-N ha^{-1} yr^{-1} above which detrimental impacts on sensitive lichen species may occur in major forests including USGS types 11 deciduous broadleaf forest, 12 deciduous needleleaf forest, 13 evergreen broadleaf, 14 evergreen needleleaf, and 15 mixed forest, and CL of 6.2 kg-N ha^{-1} yr^{-1} above which there are potential declines in community richness for herbaceous plant species including USGS types 2 dryland cropland and pasture, 3 irrigated cropland and pasture, 4 mixed dryland/irrigated cropland and pasture, 5 cropland/grassland mosaic, 6 cropland/woodland mosaic, 7 grassland, 8 shrubland, 9 mixed shrubland/grassland, and 10 Savanna. **B** Includes relative (%) difference (FIRE-NOFIRE/NOFIRE) for Nr/CL trends, where insert values pertain to Mann–Kendall (MK) scores and Theil–Sen (TS) trends across the western U.S.

agricultural, and economic damages resulting from continued climate change and related increases in fire activity and Nr emissions.

Methods

Model system and configuration

The North American chemical reanalysis (NACR): this study analyzes major meteorological, chemical, and atmospheric deposition data outputs from the North American chemical reanalysis (NACR) developed at George Mason University, which is based on a state-of-the-science, offline-coupled weather and chemical transport modelling system driven by detailed inventories of anthropogenic and natural source emissions. The meteorological simulations are downscaled from the European Centre for Medium-Range Weather Forecasts' (ECMWF) reanalysis version 5 (ERA5) (https://www.ecmwf.int/en/forecasts/dataset/ecmwf-reanalysis-v5) using the weather research and forecasting (WRF) model[26], which drives process-level simulations of the full life cycle of major air pollutants and their precursors using the U.S. EPA community scale air quality (CMAQ) model[27–29]. The NACR system used in this study includes the simulation period of 2002–2021 with a 12 × 12 km horizontal resolution WRF/CMAQ modeling domain centered over the contiguous U.S. (CONUS).

Critical to the results in this work is the use of a reliable and coherent long-term emissions dataset that includes both detailed anthropogenic and fire emissions over CONUS. The NACR simulations here use the US EPA's Air QUAlity TimE Series (EQUATES) project[2] for years 2002–2017 combined with U.S. EPA National Emissions Inventories (NEI) and related emissions modeling platforms for years 2018–2021[30–33]. The use of EQUATES and NEI emissions in the full chemistry NACR simulations allow this study to quantify the contribution of fires, particularly wildfires in the western U.S. and their impacts on long-term trends of climate and weather, Nr deposition, and resulting CL implications for terrestrial ecosystems in the U.S.

Meteorological model: The meteorological model in the NACR system is based on the WRF model V4.2[26] with a horizontal resolution of 12 km and 35 vertical layers. ECMWF's ERA-5 reanalysis data is downscaled from approximately 31 km resolution to provide initial and boundary conditions to WRF. The time step for the WRF simulation is 60 s. The main physics choices were the Grell-Freitas scheme for parameterized cumulus processes[34], the Yonsei University (YSU) scheme for the planetary boundary layer (PBL) processes[35], the two-moment Morrison microphysics for cloud physics processes[36], the RRTMG scheme for longwave and shortwave radiation[37], and the Pleim-Xiu Land Surface Model for land surface processes[38,39] (Table 1). Four-dimensional data assimilation nudging to the ERA5 meteorology is applied throughout the NACR simulation to best constrain the driving weather conditions and subsequent chemical simulations.

Chemical transport model: the meteorological and land outputs from the downscaled WRF simulations (at an hourly timestep) are processed by the U.S. EPA meteorology-chemistry interface processor (MCIP)[40] and are subsequently used to drive the chemical transport model known as the community multiscale air quality (CMAQ) model V5.3.3[27–29]. The model domain is centered on the contiguous U.S. and has the same horizontal/vertical resolution as the driving WRF simulations (i.e., 12 km with 35 vertical layers). To simulate complex chemistry in NACR, we incorporate the CB6 gas-phase chemical mechanism[41], the AERO7 aerosol module[42,43], aqueous-phase chemistry[44], sub-grid/convective and resolved cloud processes and wet deposition[45], and the M3Dry dry deposition scheme[46].

Emissions data and inputs: here, the anthropogenic and biomass burning/fire emissions are based on a blend of the EPA's Air QUAlity TimE Series (EQUATES) emissions dataset for years 2002–2017[2] and a combination of the U.S. EPA's NEI and emissions modeling platforms for 2018–2021[30–33]. For EQUATES, the emission year based on the 2017 NEI is back-projected using scaling factors based on self-consistent activity data and/or control information between the base year and projected years.

Table 1 | WRF model setup for the NACR system

Model components	
Meteorology initial and boundary conditions	ECMWF reanalysis v5 (ERA5) 31 km
Cumulus parameterization	Grell-Freitas[34]
PBL scheme	Yonsei University scheme[35]
Microphysics scheme	Two-moment Morrison microphysics[36]
Longwave and shortwave radiation	RRTMG[37]
Land surface	Pleim-Xiu land surface model[38,39]

However, for mobile source emissions (both onroad and nonroad), the Motor Vehicle Emission Simulator (MOVES) version 2014b and version 3 was used with inputs from NEI from every 3 years (i.e., 2002, 2005, 2008, 2011, 2014, and 2017). For other sources, such as electric generating units, fires, and oil and gas, available year-specific information and multiple emissions modeling platforms are used.

The sparse matrix operator kernel emissions (SMOKE) model[47] is used to process the annual, county-level inventory files using a combination of meteorological and other ancillary data (spatial, temporal, and chemical speciation information). The SMOKE results are CMAQ model-ready speciated and hourly anthropogenic and fire emissions for the CB6-AERO7 chemistry-aerosol mechanisms. Additionally, two natural source emissions are calculated inline to NACR/CMAQ: biogenic and sea salt. The biogenic emissions from vegetation/terrestrial plants are based on the CMAQv5.3.3 inline version of the biogenic emission inventory system (BEIS)[48], while the emissions of sea salt are based on inline parameterizations for sea-spray emissions[49,50].

Simulation design and outputs: here we conducted two sensitivity runs for NACR—one with fire emissions (FIRE) and one without (NOFIRE)—to assess the impact of fire emissions on Nr deposition trends in the U.S. NACR provides comprehensive outputs of all gridded Nr deposition species by different ecosystem and region, which are pivotal to the detailed assessments in this work and for ecosystem health impacts.

Further information on the WRF/CMAQ model configuration as used in NACR, as well as discussion on evaluation and uncertainties across various fire emissions inventories, related processes (e.g., fire plume rise and transport), and their impacts on air quality are available in previous studies[51,52]. These investigations demonstrate the primary importance of wildfire emissions on contributions to both gas and aerosol abundances in the atmosphere, while highlighting uncertainties that remain in these model platforms. In the next sections, we provide additional information on the analyses and evaluations of NACR, as well as address remaining uncertainties and observational gaps, placing our main results into context.

Analyses and evaluations

U.S. climate regions: to quantify the effects of fires on Nr emissions, deposition, and CLs across the U.S., we aggregate the NACR data using historical NOAA climate regions. See Supplementary Fig. S2 for delineation of the regions by state border in the U.S., which pertains to data found at NOAA's National Centers for Environmental Information[53]. These nine climatically consistent regions are useful for placing the NACR output into a historical perspective over the multi-decadal 2002–2021 period used to analyze climate, fire activity and emissions, and resulting Nr deposition trends in this work. Here we use USGS shapefiles for the state boundaries of the U.S., provided by the National Atlas of the U.S.[54].

Model trend analyses: to test the significance of climate, fire activity, and Nr deposition trends over the NACR multi-decadal time series, we calculate the Mann–Kendall (MK) nonparametric test for monotonic trend and the Theil–Sen (TS) robust estimate of linear trend)[55–57]. The MK test computes the sign of the difference between later-measured data and earlier-measured data to determine if there is a monotonic upward or downward trend in the variables of interest, while the TS robustly fits a line to the specific variable data points in the plane (i.e., a simple linear regression). This is done by calculating and then using the median of the slopes of all lines through pairs of points. The main advantage of using MK and TS compared to ordinary least squares regression methods is that it is insensitive to outliers, can be used when the data is not normally distributed, and can be more accurate.

Model evaluations and uncertainties: NACR has been evaluated for model performance in reproducing the long-term trends for both meteorological and chemical relevant variables in recent work. Overall, the NACR system can well represent the 2002–2021 trends in near-surface meteorology, such as 2-meter temperature, 2-meter mixing ratio, 10-meter wind speed, downward shortwave radiation at the surface, and total precipitation (indication of some underpredictions). Evaluation of trends in trace gases shows that the NACR simulations (both FIRE and NOFIRE) agrees very well in the long-term trends in near-surface ozone, nitrogen dioxide, and sulfur dioxide, with indication of a systematic underprediction in carbon monoxide. Evaluating the NACR fine particulate matter also demonstrates overall good agreement with observed trends, but that inclusion of fire emissions (FIRE) leads to an improved model performance compared to the NOFIRE simulation. Previous work shows that similar CMAQ model outputs of Nr wet and dry deposition species correlate well with observations during the year 2020[13].

The NACR simulations are further evaluated here for the average 2002–2021 spatial distribution and trends of NH_3 mixing ratio, HNO_3, NO_3^-, and NH_4^+ dry deposition, and NO_3^- and NH_4^+ wet deposition against ammonia monitoring network (AMoN), clean air status and trends network (CASTNET), and NADP observations, respectively (Supplementary Figs. S17 and S18). Results demonstrate that NACR FIRE simulations well capture areas of moderate to high NH_3 mixing ratios and HNO_3, NO_3^-, and NH_4^+ dry and wet deposition, especially in the western U.S.; however, there are clear areas of overpredicted HNO_3 dry deposition in the east, overpredicted NO_3^- dry deposition in coastal regions, and relatively widespread underpredictions of both NO_3^- and NH_4^+ wet deposition across most of CONUS (Fig. S17). The NACR time series indicate that the model can effectively capture the trends in NH_3 mixing ratio, and HNO_3, NO_3^-, and NH_4^+ dry and wet deposition, but that there are systematic disagreements in magnitude for the CONUS average across network sites (e.g., underpredicted NH_3 mixing ratio, NH_4^+ dry deposition, and NO_3^- and NH_4^+ wet deposition; overpredicted HNO_3 and NO_3^- dry deposition).

The underpredicted NH_3 mixing ratios are impacted by potentially missing sources of emissions in the EQUATES and NEI inputs (particularly from agriculture and mobile sources). The overpredicted HNO_3 dry deposition (dominant atmospheric removal pathway) are impacted by too rapid HNO_3 dry deposition rates in CMAQ, stemming from uncertainties in its thermodynamic calculations and chemistry, meteorological inputs from WRF, and representation of the land–surface interactions[58]. The overpredicted NO_3^- dry deposition is a result of adapting complex aerosol dry deposition schemes in CMAQ[59], as well as too high particulate NO_3^- concentrations due to linked uncertainties with upwind HNO_3 precursor concentrations (Fig. S17b) and missing chemical loss processes in the model (e.g., over water and coastal regions; Fig. S17d). The widespread underpredictions in NO_3^- and NH_4^+ wet deposition is largely due to underpredictions in NCAR predictions of total precipitation rates from WRF. While these results provide evidence of the NACR capability to generally reproduce spatiotemporal distributions of Nr concentrations and deposition, there is a need for new observations of Nr dry deposition to landscapes during smoke events and analysis of existing air quality monitoring data to better evaluate model performance in the context of fire impacts on atmospheric and ecological processes. In light of this, ultimately our work here evaluates the relative contribution of fire sources to Nr deposition in 2002–2021, which remains important in regions of the western U.S. that typically experience overall lower Nr deposition.

A previous study evaluated an ensemble of chemical transport models (including the CMAQ model) for deposition and critical load assessments against a robust suite of critical load data in North America for two

individual years, 2010 and 2016[25]. Overall, the ensemble of models all predicted a decrease in Nr critical load exceedance for terrestrial ecosystems between 2010 and 2016, which is consistent with the downward trends in our work (Figs. 3A and S7a). However, the spatial extent and magnitude of critical load exceedances varied amongst the models, and all models had annual negative biases in wet deposition compared to observations, also in agreement with our evaluations (Fig. S18e, f). Much of this uncertainty was linked to missing processes in particle nitrate dry deposition algorithms, as well as uncertainty in cuticle and soil dry deposition pathways for Nr species, such as nitric acid. This work has found also that usage of bi-directional ammonia deposition parameterizations (not used in our work for NACR) can have both a positive and negative effect on model performance and biases, which is subject to uncertainty and thus dependent on the model and bidirectional flux algorithm employed.

Data availability

All NACR 2002–2021 post-processed data and scripts used in this paper for land, meteorology, emissions, and chemistry/deposition analyses are publicly available online at: https://doi.org/10.5281/zenodo.15064964. The EQUATES dataset are available by download from the Community Modeling and Analysis System (CMAS) Data Warehouse available online at: https://www.epa.gov/cmaq/equates. National Trends Network (NTN) wet deposition data are publicly available from the National Atmospheric Deposition Program (NADP) at: https://nadp.slh.wisc.edu/networks/national-trends-network/. Data last accessed 09/24/2025. National Atmospheric Deposition Program (NRSP-3). 2022. NADP Program Office, Wisconsin State Laboratory of Hygiene, 465 Henry Mall, Madison, WI 53706. Ammonia Monitoring Network (AMoN) data are publicly available from the National Atmospheric Deposition Program (NADP) at: https://nadp.slh.wisc.edu/networks/ammonia-monitoring-network/. Data last accessed 09/24/2025. National Atmospheric Deposition Program (NRSP-3). 2022. NADP Program Office, Wisconsin State Laboratory of Hygiene, 465 Henry Mall, Madison, WI 53706. Clean Air Status and Trend Network (CASTNET) data are publicly available at: www.epa.gov/castnet. Filter pack data (https://gaftp.epa.gov/castnet/CASTNET_Outgoing/data/drydep_week_web.zip) last accessed 09/24/2025. U.S. Environmental Protection Agency, Clean Air Markets Division, Clean Air Status and Trends Network (CASTNET).

Code availability

WRFv4.2: https://github.com/wrf-model/WRF/releases/tag/v4.2 CMAQv5.3.3: https://doi.org/10.5281/zenodo.5213949. SMOKE: https://www.cmascenter.org/smoke/.

Received: 22 May 2025; Accepted: 29 January 2026;
Published online: 11 February 2026

References

1. Gruber, N. & Galloway, J. N. An Earth-system perspective of the global nitrogen cycle. *Nature* **451**, 293–296 (2008).
2. Foley, K. M. et al. 2002−2017 anthropogenic emissions data for air quality modeling over the United States. *Data Brief.* **47**, 109022 (2023).
3. EPA. Emissions inventory for air quality modeling technical support document: Heavy-duty vehicle greenhouse gas phase 2 final rule. (2016a). Retrieved from https://nepis.epa.gov/Exe/ZyPDF.cgi/P100PKEE.PDF?Dockey=P100PKEE.PDF
4. EPA. Air quality modeling technical support document: Heavy-duty vehicle greenhouse gas phase 2 final rule. (2016b). Retrieved from https://nepis.epa.gov/Exe/ZyPDF.cgi/P100PKAP.PDF?Dockey=P100PKAP.PDF.
5. Galloway, J. N. et al. The nitrogen cascade. *BioScience* **ume 53**, 341–356 (2003).
6. Phelan, J. N. et al. Climate change could negate U.S. forest ecosystem service benefits gained through reductions in nitrogen and sulfur deposition. *Sci. Rep.* **14**, 10767 (2024).
7. Bray, C. D., Battye, W. H., Aneja, V. P. & Schlesinger, W. H. Global emissions of NH3, NOx, and N2O from biomass burning and the impact of climate change. *J. Air Waste Manag. Assoc.* **71**, 102–114 (2021).
8. Bray, C. D. et al. Ammonia emissions from biomass burning in the continental United States. *Atmos. Environ.* **187**, 50–61 (2018).
9. Akdemir, E. A., Battye, W. H., Myers, C. B. & Aneja, V. P. Estimating NH_3 and $PM_{2.5}$ emissions from the Australia mega wildfires and the impact of plume transport on air quality in Australia and New Zealand. *Environ. Sci. Atmos.* **2**, 634–646 (2022).
10. Lurmann, F., Avol, E. & Gilliland, F. Emissions reduction policies and recent trends in Southern California's ambient air quality. *J. Air Waste Manag. Assoc.* **65**, 324–335 (2015).
11. McClure, C. D. & Jaffe, D. A. US particulate matter air quality improves except in wildfire-prone areas. *Proc. Natl. Acad. Sci. USA* **115**, 7901–7906 (2018).
12. Koplitz, S. N. et al. The contribution of wildland fire emissions to deposition in the U S: implications for tree growth and survival in the Northwest. *Environ. Res. Lett.* **16**, 024028 (2021).
13. Campbell, P. C. et al. Pronounced increases in nitrogen emissions and deposition due to the historic 2020 wildfires in the western U.S. *STOTEN* **839**, 156130 (2022).
14. Holguin, J., Mclaren, J. R. & Collins, S. L. Nitrogen deposition and terrestrial biodiversity. *Encycl. Biodivers.* **ume 3**, 651–671 (2024).
15. USGCRP: Fifth National Climate Assessment. Crimmins, A. R., C.W. Avery, D.R. Easterling, K. E. Kunkel, B. C. Stewart, and T.K. Maycock, Eds. U.S. Global Change Research Program, Washington, DC, USA https://doi.org/10.7930/NCA5.2023 (2023).
16. Johnson, D. W., Fenn, M. E., Miller, W. W., & Hunsaker, C. T. Fire effects on carbon and nitrogen cycling in forests of the Sierra Nevada. In: Bytnerowicz, Andrzej; Arbaugh, Michael; Andersen, Christian; Riebau, Allen 2009. Wildland Fires and Air Pollution. Developments in Environmental Science 8. 405–423 https://www.fs.usda.gov/research/treesearch/34233 (Elsevier, 2009).
17. Liao, X., Inglett, P. W. & Inglett, K. S. Fire effects on nitrogen cycling in native and restored calcareous. *Wetl. Fire Ecol.* **556**, 136–145 (2016).
18. Vasquez, K. Wildfires may alter the nitrogen cycle—and air pollution, *Eos* **102**, https://doi.org/10.1029/2021EO210647 (2021).
19. World Meteorological Organization. Fire emissions are an important source of atmospheric nitrogen deposition to downwind ecosystems. *WMO Air Quality and Climate Bulletin*, No. 3-September 2023. 7–8 https://library.wmo.int/idurl/4/62090 (2023).
20. Paul, M. J. et al. Effects of air pollutants from wildfires on downwind ecosystems: observations, knowledge gaps, and questions for assessing risk. *Environ. Sci. Technol.* **57**, 14787–14796 (2023).
21. Abatzoglou J. T. & Kolden C. A. Relationships between climate and macroscale area burned in the western United States. *Int'l J. Wildland Fire* **22**, https://doi.org/10.1071/WF13019 (2013).
22. Seager, R. et al. Climatology, variability, and trends in the U.S. vapor pressure deficit, an important fire-related meteorological quantity. *J. Appl. Meteorol*. **54**, https://doi.org/10.1175/JAMC-D-14-0321.1 (2015).
23. Melvin, M. A. National Prescribed Fire Use Report. Technical Bulletin 04-40, Prepared by the Coalition of Prescribed Fire Councils, Inc. (2020) https://www.stateforesters.org/wp-content/uploads/2020/12/2020-Prescribed-Fire-Use-Report.pdf (2025).
24. Hashida, Y., Lewis, D. J. & Cummins, K. Prescribed fires as a climate change adaptation tool. *J. Environ. Econ. Manag.* **130**, 103081 (2025).
25. Makar, P. A. et al. Critical load exceedances for North America and Europe using an ensemble of models and an investigation of causes of environmental impact estimate variability: an AQMEII4 study. *Atmos. Chem. Phys.* **25**, 3049–3107 (2025).
26. Skamarock, W. et al. A Description of the Advanced Research WRF Model Version 4.1. *UCAR/NCAR - Library.* https://n2t.org/ark:/85065/d72r3vrp (2019). Accessed 06 February 2026.

27. Byun, D. & Schere, K. L. Review of the governing equations, computational algorithms, and other components of the models-3 community multiscale air quality (CMAQ) modeling system. *Appl. Mech. Rev.* **59**, 51–77 (2006).
28. Appel, K. W. et al. The community multiscale air quality (CMAQ) model versions 5.3 and 5.3.1: system updates and evaluation. *Geosci. Model Dev.* **14**, 2867–2897 (2021).
29. US EPA Office of Research and Development. CMAQ (5.3.3). https://doi.org/10.5281/zenodo.5213949 (2021).
30. E. P. A. Technical Support Document (TSD) Preparation of Emissions Inventories for the 2019 North American Emissions Modeling Platform. EPA-454/B-22-012. August 2022 https://www.epa.gov/system/files/documents/2022-09/2019_EmisMod_TSD_August2022_1.pdf (2025).
31. EPA. 2020 National Emissions Inventory Technical Support Documentation. EPA-454/R-23-001a. March 2023 https://www.epa.gov/air-emissions-inventories/2020-national-emissions-inventory-nei-technical-support-document-tsd (2025).
32. EPA. Technical Support Document (TSD): Preparation of Emissions Inventories for the 2018v2 North American Emissions Modeling Platform. EPA-454/B-23-003. September 2023 https://www.epa.gov/system/files/documents/2024-02/2018v2_emismod_tsd_sep2023_508_0.pdf (2025).
33. EPA. Technical Support Document (TSD) Preparation of Emissions Inventories for the 2021 North American Emissions Modeling Platform. EPA-454/B-24-011. October 2024 https://www.epa.gov/system/files/documents/2024-10/2021_emismod_tsd_october2024.pdf (2025).
34. Grell, G. A. & Freitas, S. R. A scale and aerosol aware stochastic convective parameterization for weather and air quality modeling. *Atmos. Chem. Phys.* **14**, 5233–5250 (2014).
35. Hong, S.-Y., Noh, Y. & Dudhia, J. A new vertical diffusion package with an explicit treatment of entrainment processes. *Mon. Weather Rev.* **134**, 2318–2341 (2006).
36. Morrison, H., Thompson, G. & Tatarskii, V. Impact of cloud microphysics on the development of trailing stratiform precipitation in a simulated squall line: comparison of one- and two-moment schemes. *Mon. Weather Rev.* **137**, 991–1007 (2009).
37. Iacono, M. J. et al. Radiative forcing by long-lived greenhouse gases: calculations with the AER radiative transfer models. *J. Geophys. Res.* **113**, https://doi.org/10.1029/2008JD009944 (2008).
38. Pleim, J. E. & Xiu, A. Development and testing of a surface flux and planetary boundary layer model for application in mesoscale models. *J. Appl. Meteor.* **34**, 16–32 (1995).
39. Xiu, A. & Pleim, J. E. Development of a land surface model. Part I: application in a mesoscale meteorological model. *J. Appl. Meteor.* **40**, 192–209 (2001).
40. Otte, T. L. & Pleim, J. E. The meteorology-chemistry interface processor (MCIP) for the CMAQ modeling system: updates through MCIPv3.4.1. *Geosci. Model Dev.* **3**, 243–256 (2010).
41. Luecken, D. J., Yarwood, G. & Hutzell, W. T. Multipollutant modeling of ozone, reactive nitrogen and HAPs across the continental US with CMAQ-CB6. *Atmos. Environ.* **201**, 62–72 (2019).
42. Pye, H. O. et al. Modeling the current and future roles of particulate organic nitrates in the southeastern United States. *Environ. Sci. Technol.* **49**, 14195–14203 (2015).
43. Xu, L. et al. Experimental and model estimates of the contributions from biogenic monoterpenes and sesquiterpenes to secondary organic aerosol in the southeastern United States. *Atmos. Chem. Phys.* **18**, 12613–12637 (2018).
44. Fahey, K. M. et al. A framework for expanding aqueous chemistry in the community multiscale air quality (CMAQ) model version 5.1. *Geosci. Model Dev.* **10**, 1587–1605 (2017).
45. Byun, D. W. & Ching, J. K. S. Science Algorithms of the EPA Models-3 Community Multiscale Air Quality (CMAQ) Modeling System. EPA/600/R-99/030 https://cfpub.epa.gov/si/si_public_record_report.cfm?dirEntryId=63400&Lab=NERL (1999).
46. Pleim, J. & Ran, L. Surface flux modeling for air quality applications. *Atmosphere* **2**, 271–302 (2011).
47. Houyoux, M. R. et al. Emission inventory development and processing for the seasonal model for regional air quality (SMRAQ) project. *J. Geophys. Res.* **105**, https://doi.org/10.1029/1999JD900975 (2000).
48. Pierce, T. et al. Influence of increased isoprene emissions on regional ozone modeling. *J. Geophys. Res.* **103**, https://doi.org/10.1029/98JD01804 (1998).
49. Gong, S. L. A parameterization of sea-salt aerosol source function for sub- and super-micron particles. *Glob. Biogeochem. Cycles* **17**, https://doi.org/10.1029/2003GB002079 (2003).
50. Gantt, B., Kelly, J. T. & Bash, J. O. Updating sea spray aerosol emissions in the community multiscale air quality (CMAQ) model version 5.0.2. *Geosci. Model Dev.* **8**, 3733–3746 (2015).
51. Li, Y. et al. Dominance of wildfires impact on air quality exceedances during the 2020 record-breaking wildfire season in the United States. *Geophys. Res. Lett.* **48**, https://doi.org/10.1029/2021GL094908 (2021).
52. Li, Y. et al. Impacts of estimated plume rise on PM2.5 exceedance prediction during extreme wildfire events: a comparison of three schemes (Briggs, Freitas, and Sofiev). *Atmos. Chem. Phys.* **23**, https://doi.org/10.5194/acp-23-3083-2023 (2023).
53. Karl, T. R., Koss, W. J. Regional and National Monthly, Seasonal, and Annual Temperature Weighted by Area, 1895-1983. Historical Climatology Series 4-3, National Climatic Data Center, 38 pp. (1984) https://www.ncei.noaa.gov/access/monitoring/reference-maps/us-climate-regions (2025).
54. National atlas of the United States, 200506, State Boundaries of the United States: National Atlas of the United States, Reston, VA https://pubs.usgs.gov/of/2009/1151/data/basemap/statesp020faq.htm (2025).
55. Mann, H. B. Non-parametric tests against trend. *Econometrica* **13**, 245 (1945).
56. Kendall, M. G. *Rank Correlation Methods*, 4th edn. (Charles Griffin, 1975).
57. Gilbert, R. O. *Statistical Methods for Environmental Pollution Monitoring* (Wiley, 1987).
58. Shimadera, H. et al. Sensitivity analyses of factors influencing CMAQ performance for fine particulate nitrate. *J. Air Waste Manag. Assoc.* **64**, 374–387 (2014).
59. Shu Q. et al. Improving the particle dry deposition scheme in the CMAQ photochemical modeling system. *Atmos. Environ.* **289**, 119343 (2022).

Acknowledgements

The authors are grateful to the US EPA, NOAA, NCAR and their partners for providing the computer models, input data and observation data used in this study, and to Kristen Foley, James Beidler, George Pouliot, Christian Hogrefe, Wyat Appel and Kiran Alapaty of US EPA for their contributions to make the EQUATES dataset available and/or their constructive comments on earlier versions of this manuscript. This work has been financially supported by NASA Health and Air Quality Program (80NSSC22K1050), NOAA Weather Program Office (NA25OARX459C0006-T1-01), and National Institute of Environmental Health Science (1P20ES036775-01). This study was supported by NOAA Grant NA24NESX432C0001 (Cooperative Institute for Satellite Earth System Studies-CISESS) at the University of Maryland/ESSIC. The views expressed in this article are those of the author(s) and do not necessarily represent the views or policies of the US EPA, NOAA, NASA, NIEHS, USDA, or NCAR.

Author contributions

P.C.C. and D.Q.T. are the lead researchers in this study, responsible for research design, experiments, analyzing, results and writing the original manuscript. S.C., S.M., Y.L., and J.D. helped guide the research design, performed simulations, assessed model results, and reviewed the manuscript. R.S., B.B., and Y.T. helped guide research design, assessed

model results, and reviewed the manuscript. J.W. helped guide research design, assessed model results, reviewed the manuscript, and provided observational data used in model evaluation.

Competing interests
The authors declare no competing interests.

Additional information
Supplementary information The online version contains supplementary material available at https://doi.org/10.1038/s43247-026-03279-4.

Correspondence and requests for materials should be addressed to Patrick C. Campbell.

Peer review information *Communications Earth and Environment* thanks Flávio Quadros and the other anonymous reviewer(s) for their contribution to the peer review of this work. Primary handling editors: Mengze Li and Mengjie Wang. [A peer review file is available].